Journal of Power Sources 253 (2014) 201–204

Contents lists available at ScienceDirect

Journal of Power Sources

journal homepage: www.elsevier.com/locate/jpowsour

Short communication

Effects of Mo content on microstructure and corrosion resistance of arc ion plated Ti–Mo–N films on 316L stainless steel as bipolar plates for polymer exchange membrane fuel cells

Min Zhang [a,c,*], Kwang Ho Kim [b], Zhigang Shao [c,1], Feifei Wang [a], Shuang Zhao [a], Ni Suo [a]

[a] School of Physics and Electronic Technology, Liaoning Normal University, Dalian 116029, China
[b] National Core Research Center for Hybrid Materials Solution, Pusan National University, Busan 735-602, South Korea
[c] Lab of Fuel Cell System & Engineering, Dalian Institute of Chemical Physics, Chinese Academy of Sciences, Dalian 116023, China

HIGHLIGHTS

- Ti–Mo–N films were fabricated using arc ion plating combining magnetron sputtering.
- TiN film with a (111) preferred orientation shows the best corrosion resistance.
- Mo content exerts strong influence on preferred orientation of the Ti–Mo–N films.

ARTICLE INFO

Article history:
Received 7 August 2013
Received in revised form
15 December 2013
Accepted 16 December 2013
Available online 24 December 2013

Keywords:
Ternary film
Titanium molybdenum nitride
Corrosion resistance
Microstructure
Bipolar plate

ABSTRACT

Bipolar plates are one of the most important components in PEMFC stack and have multiple functions, such as separators and current collectors, distributing reactions uniformly, and etc. Stainless steel is ideal candidate for bipolar plates owing to good thermal and electrical conductivity, good mechanical properties etc. However, stainless steel plate still cannot resist the corrosion of working condition. In this work, ternary Ti–Mo–N film was fabricated on 316L stainless steel (SS316L) as a surface modification layer to enhance the corrosion resistance. Effects of Mo content on the microstructure and corrosion resistance of Ti–Mo–N films are systematically investigated by altering sputtering current of the Mo target. XRD results reveal that the preferred orientation changes from [111] to [220] direction as Mo content in the film increases. The synthesized Ti–Mo–N films form a substitutional solid solution of (Ti, Mo)N where larger Mo atoms replace Ti in TiN crystal lattice. The TiN-coated SS316L sample shows the best corrosion resistance. While Mo content in the Ti–Mo–N films increases, the corrosion resistance gradually degrades. Compared with the uncoated samples, all the Ti–Mo–N film coated samples show enhanced corrosion resistance in simulated PEMFC working condition.

1. Introduction

Polymer electrolyte membrane fuel cell (PEMFC) is a device that directly and efficiently converts chemical energy into electricity with water as the only by-product. Due to its high efficiency and near-zero emission, PEMFC is of great interest as a clean energy device beyond petroleum [1]. One of the most expensive and heaviest components in a PEMFC stack is Bipolar plate (BPP) [2], which undertakes important functions such as constituting the backbone of stack, conducting currents between cells, facilitating water and thermal management through the stack, and providing conduits for reactant gases. In order to perform these functions, the BPP should feature high corrosion resistance in PEMFC environments, good electrical conductivity, high mechanical strength, and high capability of gas separation, low cost and easily machining [3]. Stainless steel 316L (SS316L) exhibits most of the characteristics and is widely accepted as a promising BPP material [4–7]. However, its corrosion resistance is still far from satisfaction in the acidic environment of PEMFC operation. The corrosion products, such as Fe ions, tend to contaminate the catalysts and poison the proton exchange membrane, reducing the overall efficiency of the cell [8,9]. Meanwhile, the corrosion finally causes the formation of a

* Corresponding author. School of Physics & Electronic Technology, Liaoning Normal University, Dalian 116029, China. Tel.: +86 411 84379508; fax: +86 411 84379185.
E-mail addresses: m.zhang@live.com (M. Zhang), Zhgshao@dicp.ac.cn (Z. Shao).
[1] Tel.: +86 411 84379153; fax: +86 411 84379185.

0378-7753/$ – see front matter © 2013 Elsevier B.V. All rights reserved.
http://dx.doi.org/10.1016/j.jpowsour.2013.12.075

passivating layer on the stainless steel surface, which leads to an increase in ICR and a decrease in cell performance [10].

How to impart SS316L BPPs with sufficient corrosion resistance and contact conductivity inexpensively is a current hot issue. Forming a protective film on the BPPs by physical vapor deposition (PVD) is proven to be an effective method and has been extensively studied [11–16]. Ternary Ti–Me–N films are reported to exhibit superior mechanical properties and corrosion resistance to TiN films due to the addition of the third element, such as Cr [15], Al [16], etc. Mo as the addition element has been seldom reported so far.

In this work, Ternary Ti–Mo–N films were deposited on 316L stainless steel using a hybrid coating method combining arc ion plating (AIP) using Ti target and DC magnetron sputtering technique using Mo target in N_2/Ar gaseous mixture. Effects of Mo content on the microstructure and corrosion resistance of Ti–Mo–N films are systematically investigated by altering sputtering current of the Mo target.

2. Experimental

Ti–Mo–N films were deposited on 316L stainless steel substrates using a hybrid coating system, combining the arc ion plating and magnetron sputtering techniques. A schematic diagram of this apparatus was reported in the previous studies [17,18]. An arc cathode gun for Ti source and a DC-sputter gun for Mo source were installed on each side of the chamber wall. A rotational substrate holder was located on a straight line between two sources, with distances from the arc and sputter sources to the substrate being 350 and 200 mm, respectively.

2.1. Deposition

316L stainless steel (SS316L) was used as the base metal of bipolar plates. The SS316L substrates with size of 100 mm × 100 mm × 0.1 mm were ultrasonically cleaned in absolute ethyl alcohol for 15 min, and then they were polished chemically for 5 min to remove the surface oxide layer. After washed with deionized water several times, they were blown dry and put on holders.

The chamber was evacuated to a base pressure below 5.0×10^{-3} Pa using a turbo molecular pump and a rotary pump. Prior to the deposition, the substrates were cleaned again by ion bombardment using a bias voltage of −800 V under Ar atmosphere of 2.0 Pa for 15 min. Ti–Mo–N films were deposited from arc and sputter sources at a working pressure of 1.8×10^{-1} Pa. The deposition temperature was fixed at 300 °C. Typical deposition conditions for Ti–Mo–N films by the hybrid coating system are summarized in Table 1.

Table 1
Typical deposition conditions for Ti–Mo–N films prepared by hybrid coating system.

Base pressure	5.8×10^{-3} Pa
Working pressure	5.0×10^{-1} Pa
Working gas ratio	$Ar/N_2 = 1:2$
Bias voltage	−50 V
Substrate temperature	300 °C
Arc current for Ti source	65 A
Sputter current for Mo source	0–1.0 A
Deposition time	60 min
Typical coating thickness	~2 μm
Rotational velocity of substrates	25 rpm

2.2. Characterization

The film thickness was measured using a scanning electron microscopy (SEM, Hitachi, S-4200) and a stylus (α-STEP) instrument. The contents of Ti, Mo, and N in the Ti–Mo–N films were determined by an electron probe microanalyzer (EPMA, Shimadzu, EPMA-1600) operated at an accelerating voltage of 15 kV. The crystallinity of Ti–Mo–N films was analyzed with X-ray diffractometer (XRD, PANalytical, X'Pert-MPD System) using CuKα radiation. Electrochemical polarization experiments were also performed to evaluate the corrosion resistance of the samples using a potentiostat Model 2273A by EG&G Princeton Applied Research and analyzed with the corrosion software of EG&G Version 2.43.0. To simulate an aggressive PEMFC operating environment, A 0.5 M H_2SO_4 with 2 ppm F^- solution was used as the corrosive solution. A conventional three-electrode system was used in the electrochemical measurements, in which a platinum sheet acted as the counter electrode, a saturated calomel electrode (SCE, sat'd KCl) as the reference electrode and the stainless steel sample as the working electrode. The size of the working electrodes was 15 mm × 15 mm × 0.1 mm. The edges were sealed by insulating epoxy resin, only leaving a 10 mm × 10 mm surface exposed to the electrolyte. The samples were stabilized at open circuit potential (OCP) for 10 min, and then the potential was swept from the OCP in the anodic direction at a scanning rate of 20 mV s^{-1}.

3. Results and discussion

3.1. Film composition

Fig. 1 shows the compositional changes of Ti, Mo, and N in the films as a function of the Mo target current at a fixed Cr arc current of 55 A. As the Mo target current increases from 0 to 1.0 A, the Mo content in the Ti–Mo–N film increases almost linearly from 0 to 28.0 at%, with a corresponding decrease of Cr from 56.1 to 31.5 at%. The nitrogen content shows a minor fluctuation around 40 at%.

3.2. XRD results

Fig. 2 presents XRD patterns of Ti–Mo–N films with different Mo contents. For the Ti–Mo–N film deposited without Mo, the film mainly consists of TiN phase with the peaks from (111) and (311) plane and shows a preferred orientation of [111] direction. Only a peak corresponding to (211) plane from Ti_2N phase occurs at 51°.

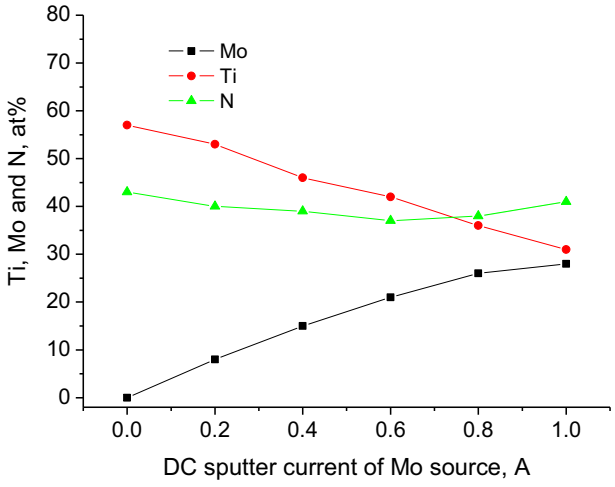

Fig. 1. Composition variation of Ti–Mo–N films as a function of sputter current of Mo.

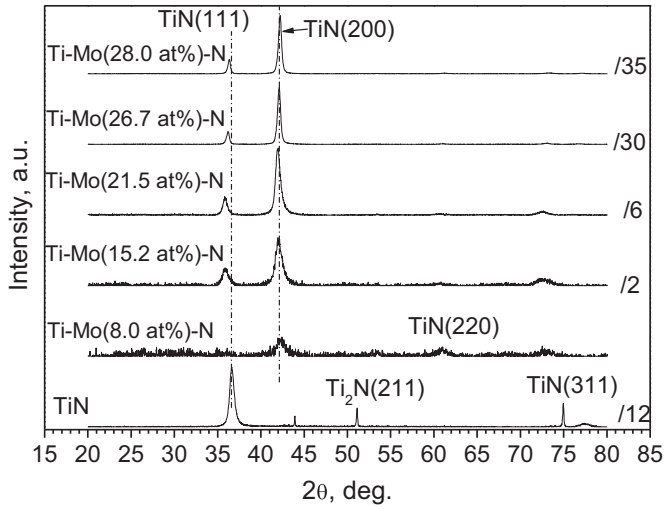

Fig. 2. XRD patterns of Ti–Mo–N films with different Mo contents.

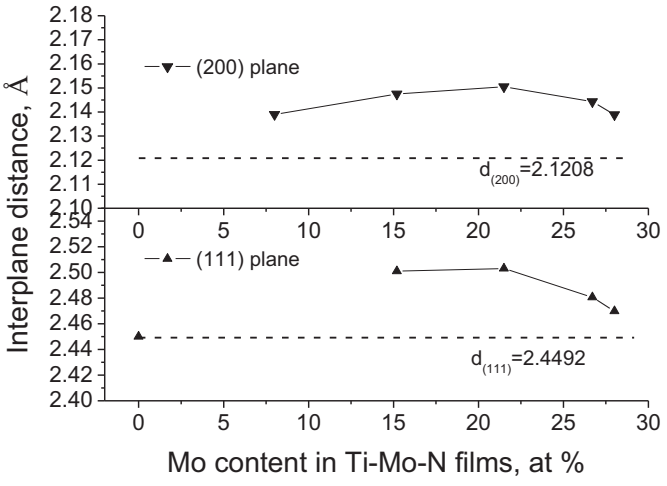

Fig. 4. Interplanar distance of TiN (111) and (200) plane as a function of Mo content.

When Mo content increases to 8.0 at%, the peaks from TiN (111), (311) and Ti_2N (211) disappear. The peaks corresponding to TiN (200) and (220) planes appear. When Mo content increases further, the intensity of TiN (200) peak increases gradually. Meanwhile, the peak corresponding to TiN (111) plane appears again and grows with Mo content gradually as well. Despite of this, the Ti–Mo–N films with Mo content more than 15.2 at% show an apparent preferred orientation at (200) plane. That is to say, the preferred orientation of the Ti–Mo–N films changes from [111] to [200] direction when the Mo content increases. It can also be seen that the (111) and (200) peaks shifted toward the lower angle when Mo content in the Ti–Mo–N films increases. We ascribe it to the substitutional solid solution of Mo atoms into TiN films.

Fig. 3 presents the dependence of crystal size on sputtering current of Mo source. The crystal size is calculated from (111) and (200) peak using $D = 0.9\lambda/B\cos\theta$, which is well known as Scherrer equation. It can be seen from Fig. 3 that crystal size calculated from either (111) or (200) plane is less than 30 nm, indicating that the films consist of nanocrystal grains. We can also figure out that the crystal size increases with raising the Mo content.

Fig. 4 shows the interplanar distance of TiN (200) and (111) crystal plane, $d_{(200)}$ and $d_{(111)}$ as a function of Mo content obtained

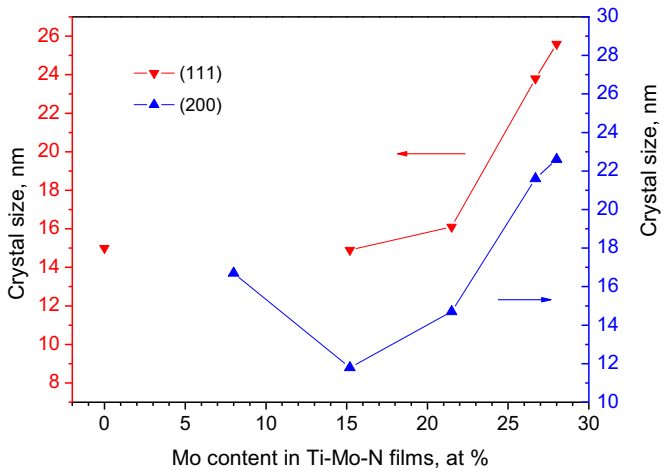

Fig. 3. The dependence of crystal size on sputtering current of Mo source.

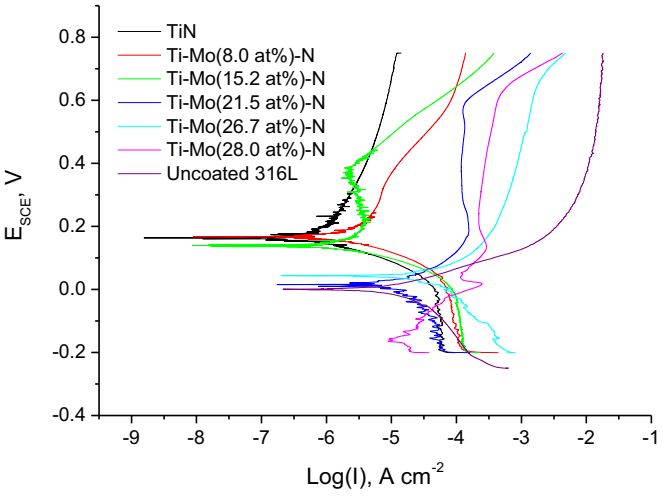

Fig. 5. The potentiodynamic polarization curves of the uncoated and coated SS316L plates with Ti–Mo–N films with different Mo contents in simulated PEMFC working solution.

from Fig. 2. The dashed lines indicate the calculated value of $d_{(200)}$ and $d_{(111)}$ for the TiN powder from JCPDS No. 38-1420 [JCPDS, X-ray Index Cards, 38-1420.]. It can be seen that the $d_{(111)}$ value of TiN film obtained in this work equals to the value of the TiN powder. Upon the addition of Mo in the Ti–Mo–N films, the $d_{(111)}$ values are higher than that of the TiN film and powder, which is attributed to larger atomic size of Mo. For the case of (200) plane, a similar phenomenon appears. In short, we can conclude that the Ti–Mo–N films obtained in this work are substitutional solid solutions of (Ti, Mo)N.

3.3. Corrosion resistance

Fig. 5 shows the potentiodynamic polarization curves of the uncoated and coated SS316L plates with Ti–Mo–N films with different Mo contents in simulated PEMFC working solution. One can see that the TiN film without Mo exhibits the highest corrosion potential and the lowest corrosion and passivation current density, about 0.16 V, $10^{-6.3}$ A cm^{-2}, and 10^{-5} A cm^{-2} respectively,

indicating the best corrosion resistance. When Mo content increases to 8.0 at%, the Ti–Mo–N film remains the same corrosion potential with the TiN film, but the corrosion and passivation current density increases to $10^{-5.8}$ A cm^{-2} and $10^{-3.6}$ A cm^{-2} respectively. When Mo content increases further from 15.2 to 21.5 and 26.7 at%, the corrosion potential decreases gradually, from 0.13 V to 0.04 and 0 V; corrosion current density increases from $10^{-5.7}$ A cm^{-2} to $10^{-5.0}$ and $10^{-4.5}$ A cm^{-2}, which is close to that of the uncoated SS316L plate. When Mo content reaches 28.0 at%, the corrosion potential declines to −0.19 V, although corrosion current density shows no apparent increase. It should be noteworthy that the passivation current density of all the coated samples is lower than that of the uncoated SS316L sample, suggesting that the coated samples undergo a much slower corrosion process than the uncoated sample in the harsh PEMFC working condition.

In short, the corrosion resistance of the Ti–Mo–N films degrades with the increase of Mo content. The Ti–Mo–N films with Mo content no more than 26.7 at% show better corrosion resistance than the uncoated SS316L sample, indicating that the Ti–Mo–N films synthesized by the present hybrid coating system are promising candidates for protecting layer on bipolar plates used in PEMFCs.

4. Discussion

It is not difficult to find that TiN films without Mo addition show a preferred orientation along (111) atomic plane and exhibit the best corrosion resistance. The Ti-0 at%Mo–N films obtained in this work show a preferred orientation at (111) plane, i.e., most crystalline grains within the films grow along the (111) atomic plane which is parallel to film surface and exposed to the outside. TiN crystal is with face-centered cubic (FCC) structure and the (111) plane is the most closed-packed plane in FCC crystals. Materials with a preferred orientation along the most closed-packed plane generally show the highest resistance against elastic deformation and electrochemical corrosion, which refer to the highest hardness value and the best corrosion resistance. This explains Ti–Mo–N films with zero addition of Mo show the best corrosion resistance.

The other point we can figure out from this work is that the addition of Mo fails to enhance the corrosion resistance, instead degrades it. Two aspects contribute to this phenomenon. Firstly, metallic molybdenum is not good at resisting corrosion by acid or saline electrolyte. Secondly, Ti–Mo–N films form in solid solution structure with single TiN phase, instead of the nanocomposite microstructure as described in our previous study [19]. The former, to some extent, destroys the integrity of TiN crystalline lattice and brings dislocation and internal stress in, definitely leading to degradation in corrosion resistance.

Despite of this, a useful suggestion can be concluded that for the TiN film with single phase, to fabricate the films with a preferred orientation along (111) atomic plane by regulating experimental parameters is helpful to enhance corrosion resistance.

5. Conclusions

Ternary Ti–Mo–N films were deposited on 316L stainless steel employing a hybrid coating method of arc ion plating (AIP) using Ti target and DC magnetron sputtering technique using Mo target in N_2/Ar gaseous mixture. Effects of Mo content up to 28.0 at% on the microstructure and corrosion resistance of Ti–Mo–N films are investigated in this study. As the Mo target current increases from 0 to 1.0 A, the Mo content in the Ti–Mo–N film increases almost linearly from 0 to 28.0 at% and the preferred orientation of the Ti–Mo–N film changes from [111] to [200] direction. The synthesized Ti–Mo–N films form a substitutional solid solution of (Ti, Mo)N where larger Mo atoms replace Ti in TiN crystal lattice. The TiN coated SS316L sample shows the best corrosion resistance (corrosion potential and current density at 0.16 V and $10^{-6.3}$ A cm^{-2} respectively), when Mo content in the Ti–Mo–N films increases the corrosion resistance gradually degrades. Compared with the uncoated samples, all the Ti–Mo–N film coated samples show enhanced corrosion resistance in simulated PEMFC working condition.

Acknowledgments

This work was financially supported by National Natural Science Foundation of China (Grant No. 51101080), Program for Liaoning Excellent Talents in University (Grant No. LJQ2011115) and the China Postdoctoral Science Foundation (Grant No. 20110491545).

References

[1] B.C.H. Steele, A. Heinzel, Nature 414 (2001) 345–346.
[2] A. Kumar, J. Power Sources 129 (2004) 62–67.
[3] H.-Y. Jung, S.-Y. Huang, P. Ganesan, B.N. Popov, J. Power Sources 194 (2009) 972–975.
[4] H. Wang, M.A. Sweikart, J.A. Turner, J. Power Sources 115 (2003) 243–251.
[5] M. Zhang, B. Wu, G. Lin, Z. Shao, M. Hou, B. Yi, J. Power Sources 196 (2011) 3249–3254.
[6] M. Zhang, G. Lin, B. Wu, Z. Shao, J. Power Sources 205 (2012) 318–323.
[7] H. Wang, J.A. Turner, Fuel Cells 10 (2010) 510–519.
[8] M.J. Kelly, G. Fafilek, J.O. Besenhard, H. Kronberger, G.E. Nauer, J. Power Sources 145 (2005) 249–252.
[9] R.A. Antunes, M.C.L. Oliveira, G. Ett, V. Ett, Int. J. Hydrogen Energy 35 (2010) 3632–3647.
[10] H. Tawfik, Y. Hung, D. Mahajan, J. Power Sources 163 (2007) 755–767.
[11] Y. Fu, G. Lin, M. Hou, B. Wu, H. Li, L. Hao, Z. Shao, B. Yi, Int. J. Hydrogen Energy 34 (2009) 453–458.
[12] B. Wu, G. Lin, Y. Fu, M. Hou, B. Yi, Int. J. Hydrogen Energy 35 (2010) 13255–13261.
[13] J. Barranco, F. Barreras, A. Lozano, M. Maza, J. Power Sources 196 (2011) 4283–4289.
[14] B.-C. Cha, Y.-Z. You, S.-T. Hong, J.-H. Kim, D.-W. Kim, B.-S. Lee, S.-K. Kim, Int. J. Hydrogen Energy 36 (2011) 4565–4572.
[15] H.S. Choi, D.H. Han, W.H. Hong, J.J. Lee, J. Power Sources 189 (2009) 966–971.
[16] L. Wang, D.O. Northwood, X. Nie, J. Housden, E. Spain, A. Leyland, A. Matthews, J. Power Sources 195 (2010) 3814–3821.
[17] S.R. Choi, I.-W. Park, S.H. Kim, K.H. Kim, Thin Solid Films 447–448 (2004) 371–376.
[18] K.H. Kim, E.Y. Choi, S.G. Hong, B.G. Park, J.H. Yoon, J.H. Yong, Surf. Coat. Technol. 201 (2006) 4068–4072.
[19] M. Zhang, L. Hu, G. Lin, Z. Shao, J. Power Sources 198 (2012) 196–202.